Supplementary Information for:

Nucleation products of ligated nanoclusters unaffected by temperature and reducing agent

John M. Pettibone and Nicole R. Reardon

Experimental Methods

All chemicals and solvents were purchased from Sigma-Aldrich and used as delivered.[1] For the Au-PPh$_3$ system, 15.0 mg (30 μmol) of Au(PPh$_3$)Cl (99.9%), were dissolved in a 20 mL borosilicate, crimp-seal vial containing either methanol-chloroform or methanol-diethyl ether (1:1, v/v). Subsequently, the addition of 5x molar excess of dry reducing agent, either borane tertbutylamine complex (BTBC) or NaBH$_4$, was added to the vial while stirred with a magnetic stir bar and crimp-sealed immediately after the addition of reducing agent to optimize initial mixing. The Au-L^3 reaction solutions contained 0.015 g (30 μmol) of Au(PPh$_3$)Cl and 12.5 mg (30 μmol) L^3, L^3 = 1,3-bis(diphenylphosphino)pentane, dissolved in the same solvent mixtures. All reaction solutions were covered with aluminum foil to minimize light exposure. The uncertainties (2σ) associated with the masses of the AuClPPh$_3$ and ligands are ±0.0002 g, resulting in an average 3% uncertainty.

Details of the colorimetric assay have been reported elsewhere.[2] Briefly, the colorimetric assay probes ionic and neutral PPh$_3$-containing Au$_8$ and Au$_9$ clusters in solution by the addition of excess assay reagent, L^3. The addition of the assay reagent promotes etching of PPh$_3$-protected Au$_8$ and Au$_9$ clusters to form [Au$_6$L$^3_4$]$^{2+}$. The addition of L^3 minimizes further reactions by trapping Au^I in [AuL$^3_2$]$^+$ through ligand exchange, lowering the rate of reduction of Au^I to a near null rate. [Au$_6$L$^3_4$]$^{2+}$ has an optical signature in the UV-Vis centered at 585 nm and the conversion is nearly ideal. The relative intensity of 585 nm band is quantitatively representative of (almost) the entire PPh$_3$-containing Au$_8$ and Au$_9$ clusters present. Furthermore, the distribution of larger nanocluster species, {Au$_x$: $x > 9$}, can be narrowed to smaller clusters and probed by their characteristic UV-Vis bands, {Au$_x$: $10 \leq x \leq 13$}. Nanoclusters that are not able to be etched back to Au$_x$, $x < 14$, cannot be uniquely identified, but relative intensities of peaks probed can provide information about the evolution of the cluster distribution. At each time point, 0.6 mg ± 0.01 mg of reaction solution were weighed and added through a septum to 2.0 mL of methanol and 0.5 mL of 3x molar excess L^3 (90 μmol) stock solution. The solutions were covered with aluminum foil and mixed for 24 h. Importantly, all methanol solutions were purged with Ar. Each reaction solution and assay solution contain the same concentration of gold and L^3 so all intensities can be compared quantitatively. Evaluation of assay solutions with strong scattering due to larger particles were modeled based on Rayleigh scattering. The reactions conducted at 0 °C were housed in a temperature controlled cooling unit. The metal-ligand solutions were allowed to equilibrate overnight prior to the addition of the reducing agent. Thermocouple readings were ± 1 °C throughout the experiment. The sealed reaction vials were secured to minimize handling during sample collection.

Molar ratios of diphosphine ligands and AgNO$_3$ were also examined as function of the carbon backbone chain in the diphosphine ligands. As stated previously, we notate diphosphine ligands as L^n, where L^n = 1,n-bis(diphenylphosphino) n-alkane. All reactions were conducted in methanol-chloroform (1:1, v/v) solutions.

Dynamic light scattering (DLS) measurements were conducted using a Malvern Zetasizer Nano ZS equipped with a 4 mW 633 nm laser. DLS measurements were conducted on assayed solutions prepared in 1:1 methanol:diethyl ether (Sigma Aldrich, CHROMASOLV, 99.9%, inhibitor free). Prior to the addition of the precursor reagents, the methanol was passed through a 0.2 μm filter to remove dust. Background measurements were conducted on solutions containing dissolved ligands, Au(PPh$_3$)Cl alone, reducing agent alone dissolved for

more than 1 h in the solvent system, and dissolved reducing agents and ligands together; these measurements exhibited null results, providing evidence that the DLS distributions derived for reaction solutions represent only reduced gold nanoparticles. Similar experimental procedure was used for the L^n-AgNO$_3$ system, but 100 μL of reaction solution were diluted into 3 mL of chloroform.

ESI-MS data were obtained in negative and positive ion modes. The mass spectrometer comprised an electrospray ion source (Analytica of Branford), coupled to a custom-built (by Ardara Technologies) Extrel CMS quadrupole mass spectrometer. Samples were introduced to the ESI source via direct infusion (5 μL/min) through a glass capillary and were purged with pure methanol between each sample. The source electrical potentials, temperature, curtain gas flow, and effusion rate were optimized to maximize ion intensities while minimizing fragmentation. To minimize bias, spectra were systematically collected for voltages between 80 V and 175 V.

Nanoparticle light scattering

We examine the contribution from scattering in the extinction spectra observed in the assayed solutions by using simulated Rayleigh scattering, where a constant refractive index is assumed for all gold scattering species examined. For Rayleigh scattering, the intensity of scattered light from hard spheres is proportional to the incident wavelength, λ^{-4}, and particle radius, r^6. Because scattering intensity is proportional to r^6, the scattering intensity will likely be dominated by the largest scattering gold species present. Subsequently, the relative change in the scattering sphere diameter can be monitored and approximated by $r_2/r_1 \approx C^{1/6}$, where r_1 and r_2 are the radii of the two scattering spheres and C is the ratio of the scattered intensities, I_i, assuming that the optical properties of the nanoparticles are the same.

Because scattering was clearly observed in the Au-PPh$_3$ system and not evident in the Au-L^3 system, we examined the assayed Au-L^3 and Au-PPh$_3$ solutions with dynamic light scattering (DLS) to provide further evidence that the colorimetric assay efficiently probes the product distribution (not shown). In the Au-PPh$_3$ assayed solutions that contain characteristic scattering of larger species, the DLS measurements are capable of detecting nanoparticles. The resulting intensity distribution is broad due to the particle size being at the edge of the detection limit for the instrument. The volume distribution provides evidence of a large gold population with hydrodynamic diameters near 1 nm. However, the Au-L^3 systems do not have distinct scattering signatures in the assayed solutions and also provide no signal in DLS, consistent with the absence of nanoparticles.
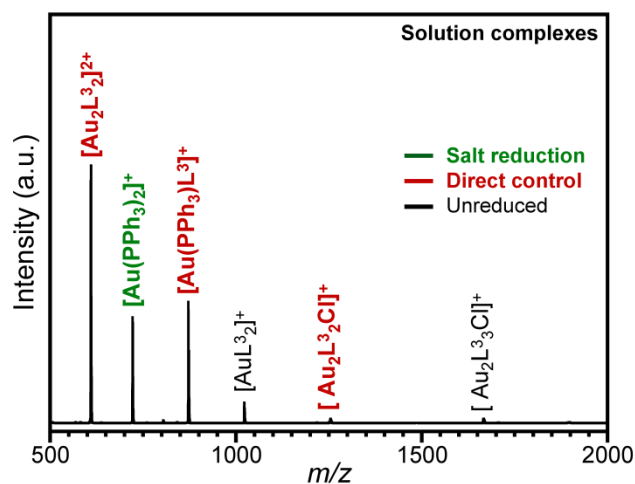
Figure S1. Distribution of complexes present in solution resulting from equimolar concentrations of $AuClPPh_3$ and L^3. The reduction rate of $[Au(PPh_3)_2]^+$ (green) is faster than complexes containing L^3, resulting in different rates of reduction at lower temperatures and slower reducing rates (BTBC). The products from only the reduction of $[Au(PPh_3)_2]^+$ and $AuClPPh_3$ result in a broad distribution of products, which are similar to initial product distributions reported for other metal salt reductions. The reduction of complexes containing diphosphine ligands result in the direct formation of a *uniform* population of ligated Au_8 and Au_9 clusters.
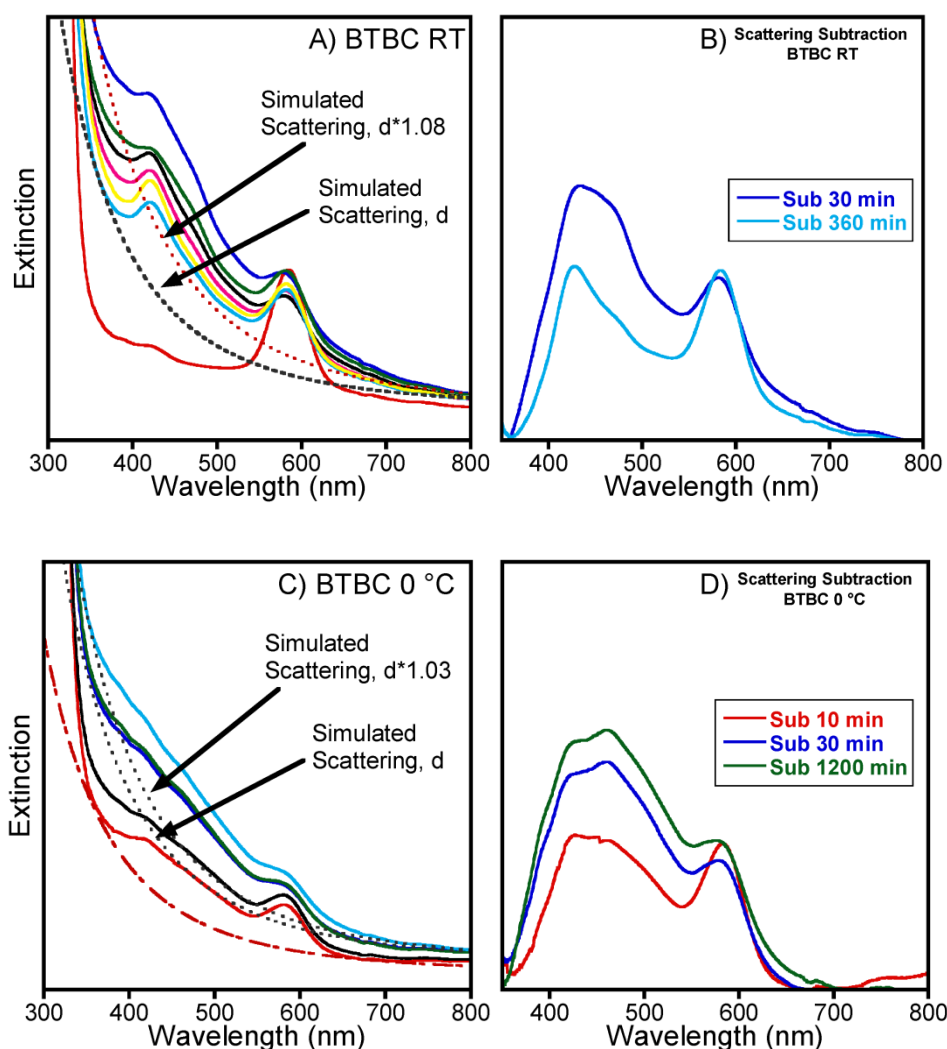
Figure S2. A) Simulated Rayleigh scattering curves (dashed line) overlaid on the room temperature (20 °C) BTBC reduced Au-PPh$_3$ system extinction spectra. B) Subtraction of the scattering from the extinction spectra of Au-PPh$_3$ systems at $t = 30$ min and 360 min. The change in the fitted simulated scattering, assuming constant optical properties, is representative of an ~ 8% change in particle diameter. The decrease in the intensity of scattering is characteristic of size-selective solution processing. C) Simulated Rayleigh scattering curve (dashed line) overlaid on the 0 °C BTBC reduced Au-PPh$_3$ system that was subtracted from all Au-PPh$_3$ extinction spectra at $t = 10$ min, 30 min, and 1200 min. D) The subtracted extinction spectra from the assayed solutions. The difference of the simulated species present in the solution at $t = 30$ min and 1200 min is ~ 3%. The contribution of the bands at 420 nm and 585 nm is more clearly presented with the subtraction of scattering, providing clear evidence of the latent band at 420 nm at 30 min and 1200 min.
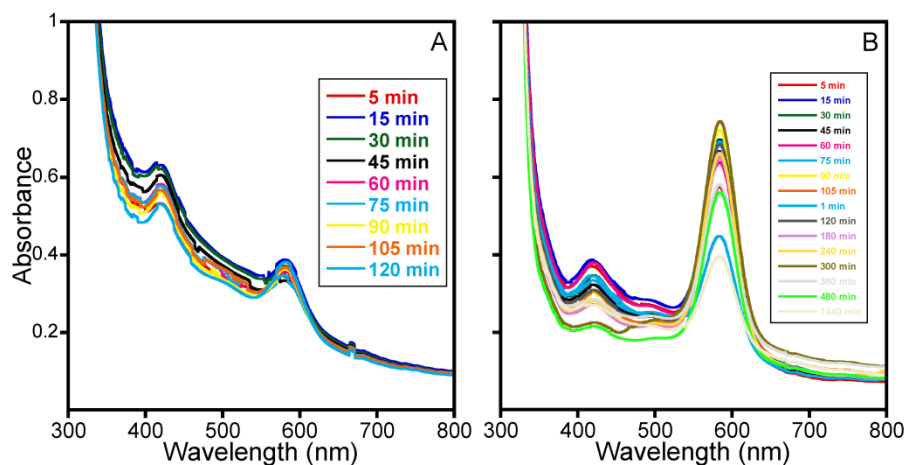
Figure S3. Colorimetric assay of the methanol-chloroform (1:1, v/v) solutions containing equimolar A) Au-PPh$_3$ and B) Au-L^3 systems at room temperature (20 °C) reduced with NaBH$_4$. Scattering is present at $t = 5$ min in Au-PPh$_3$ system and absent in Au-L^3 system, consistent with systems reduced with BTBC.
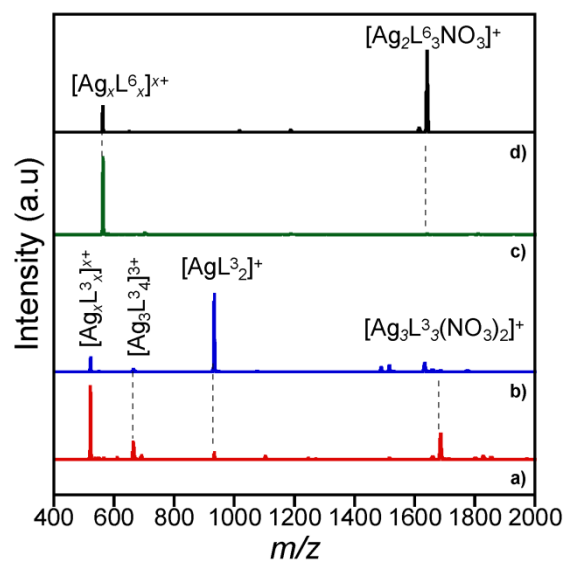
Figure S4. Distribution of cationic complexes observed for different [L^n]/[AgNO$_3$] in methanol-chloroform solutions (1:1, v/v): a) [L^3]/[AgNO$_3$] ~ 1.0, b) [L^3]/[AgNO$_3$] ~ 2.0, c) [L^6]/[AgNO$_3$] ~ 1.0, and d) [L^6]/[AgNO$_3$] ~ 2.0. Increasing the relative L^n concentration significantly changes the distributions of complexes present in solution, similar to Au^I. The increasing intensity of [Ag$_x$L^n_x]$^{x+}$ in the mass spectra results in nucleation products comprising ligated nanoclusters immediately after Ag$^+$ reduction, which do not subsequently aggregate into larger species over the time period examined. The reduction of [Ag(PPh$_3$)$_2$]$^+$ results in a broad distribution of nucleation products that includes species with characteristic plasmon bands, nanoparticles. No complexes are observed with ESI-MS in negative ion mode.

Figure S5. Representative solutions of $[PPh_3]/[AgNO_3] = 1.0$ (vial 1) and 2.0 (vial 2) at $t \approx 48$ h after $NaBH_4$ addition. Further solution phase processing in the Ag-PPh_3 systems results in larger silver species, indicated by the dark grey sediment at the bottom of both vials. Sedimentation is not observed in any Ag-L^n solutions examined.

References

1 Certain commercial materials and equipment are identified in this paper in order to adequately specify the experimental procedure. Such identification neither implies recommendation or endorsement by the National Institute of Standards and Technology nor does it imply that the material or equipment identified is the best available for the purpose.

2 J. M. Pettibone; J. W. Hudgens. *ACS Nano* 2011, **5**, 2989.